

# Illusory Attacks: Detectability Matters in Adversarial Attacks on Sequential Decision-Makers

Tim Franzmeyer<sup>1</sup> Stephen McAleer<sup>1</sup> João F. Henriques<sup>1</sup> Jakob N. Foerster<sup>1</sup> Philip H.S. Torr<sup>1</sup>  
Adel Bibi<sup>1</sup> Christian Schroeder de Witt<sup>1</sup>

## Abstract

Autonomous agents deployed in the real world need to be robust against adversarial attacks on sensory inputs. Robustifying agent policies requires anticipating the strongest attacks possible. We demonstrate that existing observation-space attacks on reinforcement learning agents have a common weakness: while effective, their lack of temporal consistency makes them *detectable* using automated means or human inspection. Detectability is undesirable to adversaries as it may trigger security escalations. We introduce *perfect illusory attacks*, a novel form of adversarial attack on sequential decision-makers that is both effective and provably *statistically undetectable*. We then propose the more versatile  $\mathcal{E}$ -illusory attacks, which result in observation transitions that are consistent with the state-transition function of the environment and can be learned end-to-end. Compared to existing attacks, we empirically find  $\mathcal{E}$ -illusory attacks to be significantly harder to detect with automated methods, and a small study with human subjects<sup>1</sup> suggests they are similarly harder to detect for humans. We conclude that future work on adversarial robustness of (human-)AI systems should focus on defences against attacks that are hard to detect by design.

## 1. Introduction

Deep reinforcement learning algorithms (Mnih et al., 2015; Schulman et al., 2017; Haarnoja et al., 2018; Salimans et al., 2017) have been applied to numerous sequential decision-making problems, ranging from recreational games (Bakhtin et al., 2022), to robotics (Todorov et al., 2012; Andrychowicz et al., 2020) and nuclear fusion (Degraeve et al., 2022).

<sup>1</sup>University of Oxford, UK. Correspondence to: Tim Franzmeyer <frtim at robots dot ox dot ac dot uk>.

<sup>1</sup>Ethical approval under reference R84123/RE001

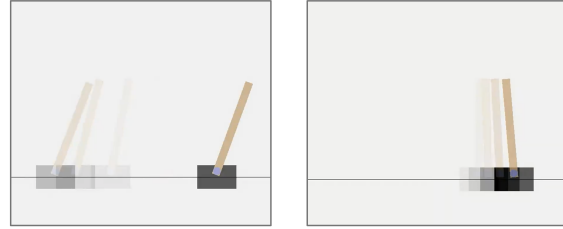


Figure 1: The left image shows an observation sequence (older observations are faded out) as seen under a state-of-the-art adversarial attack. One easily classifies this sequence as *adversarially attacked* as the cart appears to jump horizontally, violating the transition dynamics of the unattacked system. The sequence in the image on the right, resulting from our proposed *illusory attacks*, appears unsuspecting.

However, the susceptibility of deep neural networks to adversarial attacks poses threats to their safety-critical application (Kos & Song, 2017; Huang et al., 2017). This motivates research into strong adversarial attacks and robustification against them (Zhang et al., 2020; Sun et al., 2021; Liang et al., 2022).

Autonomous AI systems deployed to the real world often feature a combination of both automated and human monitoring. In practice, strong adversarial attackers will seek to evade detection as attacked agents might have access to contingency options, such as executing an emergency shutdown or triggering security escalations (Cazorla et al., 2018). Previous frameworks in observation-space adversarial attacks on sequential-decision makers often do not investigate detectability, neither through automated means nor through human inspection.

We argue that detectability should be taken into account for robustifying real-world AI systems, and further *human-AI interaction or human-in-the-loop* systems. We also investigate attacks that are not subject to perturbation budget constraints. Instead, we learn from past security incidents where an attacker fed unsuspecting pre-recorded input to surveillance cameras, or an industrial control panel (Langner, 2011, STUXNET 417 attack).

In this paper, we first construct simple automated detectors and empirically show that these can detect state-of-the-art adversarial attacks with high probability across a variety of simulated environments. Such automated detectors merely require victim agents to have access to a (possibly approximate) model of the state-transition function. Access to such *world models* is a common assumption in autonomous systems literature (Ha & Schmidhuber, 2018; Sutton, 2022), e.g. world models can be learned from train-time experience.

Likewise, we show that humans can detect state-of-the-art attacks through visual inspection (see Figure 1 for an illustration). We proceed by investigating novel classes of adversarial attacks that are harder to detect for humans and automated methods, or indeed undetectable. We first propose *perfect illusory attacks*, a novel class of *provably statistically undetectable* adversarial attacks, and implement these in various benchmark environments. However, we prove perfect illusory attacks do not exist in all environments. We then introduce the more versatile  $\mathcal{E}$ -illusory attacks, which feature a relaxed optimisation objective that encourages the resultant action-observation histories to be consistent with the state-transition function of the unattacked environment.

We empirically confirm that  $\mathcal{E}$ -illusory attacks can be efficiently learned, and – in comparison to state-of-the-art attacks – are much harder to detect, both for automated detectors based on world models and for humans. As we empirically find that existing robustification methods are largely ineffective against  $\mathcal{E}$ -illusory attacks, we suggest that the existence and effective usage of *reality feedback*, i.e., observation channels that are hardened against adversarial interference, may play a decisive role in certifying the safety of real-world AI, and human-AI, systems.

Our work makes the following contributions:

- We demonstrate that state-of-the-art adversarial attacks are reliably detected both with simple automated detectors and by human inspection.
- We formalise *perfect illusory attacks*; a novel framework for statistically undetectable adversarial attacks (see Section 4.3) and give examples in common benchmark environments in Section 5.
- We introduce  $\mathcal{E}$ -illusory attacks, a computationally feasible learning algorithm for adversarial attacks which result in action-observation sequences aligned with the state-transition function of the unperturbed environment (see Section 4.5).
- We show that, compared to state-of-the-art adversarial attacks,  $\mathcal{E}$ -illusory attacks are significantly less likely to be detected by victims with simple automated detectors (Section 5.3), as well as by humans (Section 5.4).

## 2. Related work

The **adversarial attacks** literature originates in image classification (Szegedy et al., 2013), where the goal is to find perturbations  $\delta$  for a given classifier  $f$  such that  $f$  yields different predictions for  $x$  and  $x + \delta$ , despite the difference between  $x$  and  $x + \delta$  being imperceptible to humans. To enforce the imperceptibility requirement, such works use simple minimum-norm perturbation constraints as a proxy (Goodfellow et al., 2014).

This line of work has been extended to adversarial attacks on **sequential decision-making agents** largely building upon the minimum-norm perturbation (MNP) framework (Chen et al., 2019; Ilahi et al., 2021; Qiaoben et al., 2021). In the MNP framework, the adversary can modify the victim’s observations up to a step- or episode-wise perturbation budget.

This line of work has not only examined the classical white-box attacks, but also **black-box attacks**. Zhang et al. (2020) and Sun et al. (2021) use reinforcement learning to learn adversarial policies that require only black-box access to the victim’s policy. Assuming a different black-box setting, Husenot et al. (2019) introduces a class of adversaries for which a unique mask is precomputed and added to the agents’ observation at every time step. Our framework differs from these previous works in that it takes into account the temporal consistency of observation sequences and assumes that victim agents possess detection mechanisms.

Another body of work focuses on **detecting adversarial attacks**. For example, Lin et al. (2017) develop an action-conditioned frame module that allows agents to detect adversarial attacks by comparing both the module’s action distribution with the realised action distribution. Tekgul et al. (2021) detect adversaries by evaluating the feasibility of past action sequences. There exists only a limited body of literature on **undetectable** adversarial attacks (Li et al., 2019; Sun et al., 2020; Huang & Zhu, 2019) on sequential-decision-making agents, none of which achieves statistical indistinguishability, nor takes into account temporally-extended observation dependencies. In cybersecurity, related ideas have been explored for sensor attacks on linear control systems (Mo & Sinopoli, 2010; Pasqualetti et al., 2015). Compared to these works, our proposed methods consider stronger notions of detectability, and how to *learn* attacks that are undetectable.

Work towards **robust agents in sequential decision environments** uses randomized smoothing (Kumar et al., 2021; Wu et al., 2021), test-time hardening by computing confidence bounds (Everett et al., 2021), training with adversarial loss functions (Oikarinen et al., 2021), and co-training with adversarial agents (Zhang et al., 2021; Dennis et al., 2020; Lanier et al., 2022). We compare against and build upon this line of work.

### 3. Background and notation

We denote a probability simplex over a set  $\mathcal{X}$  as  $\mathcal{P}(\mathcal{X})$ , and an unnamed probability distribution as  $\mathbb{P}(\cdot)$ . The empty set is denoted by  $\emptyset$ , and the unit impulse as  $\delta(\cdot)$ .

**MDP.** A Markov decision process (Bellman, 1958, MDP) is a tuple  $\langle \mathcal{S}, \mathcal{A}, t, r, \gamma \rangle$ , where  $\mathcal{S}$  is a discrete or continuous state space,  $\mathcal{A}$  is a discrete or continuous action space,  $t : \mathcal{S} \times \mathcal{A} \mapsto \mathcal{P}(\mathcal{S})$  is the (probabilistic) state-transition function,  $r : \mathcal{S} \times \mathcal{A} \times \mathcal{S} \mapsto \mathcal{P}(\mathbb{R})$  is a reward function, and  $\gamma \in [0, 1]$  is a scalar discount factor. Given an agent with policy  $\pi : \mathcal{S} \mapsto \mathcal{P}(\mathcal{A})$ , an MDP proceeds by sampling an initial state  $s_0 \sim t(\cdot|\emptyset) \in \mathcal{S}$ , upon which the agent observes  $s_0$ , takes an action  $a_0 \sim \pi(s_0) \in \mathcal{A}$  triggering a state transition  $s_1 \sim t(\cdot|s_0, a_0)$  and returning a reward  $r_0 \sim r(\cdot|s_0, a_0, s_0)$ . Note that, for convenience, we here subsume the initial state distribution of the MDP into its state-transition function  $t$ . Here,  $\pi : \mathcal{S} \times \mathcal{A} \rightarrow [0, 1]$  is a stochastic policy. We further define a trajectory of length  $n$  as  $\tau = (s_0, a_0, \dots, s_n)$ , and the distribution over trajectories generated by a policy  $\pi$  acting in an MDP  $\mathcal{E}$  as  $\mathbb{P}_{\mathcal{E}, \pi}(\tau)$ . In line with standard literature (Zhang et al., 2020; Ilahi et al., 2021), we assume that agents do not have access to the reward signal at test time and therefore do not include the reward signal in the trajectory. For simplicity, we only consider finite episodes of length  $T \in \mathbb{N}_+$ .

**Observation-space adversarial attacks.** Observation-space adversarial attacks consider the scenario where an *adversary* manipulates the observation of a *victim* at test-time. Much prior work falls within the SA-MDP framework (Zhang et al., 2020), in which a state-adversarial agent with policy  $\nu : \mathcal{S} \mapsto \mathcal{P}(\mathcal{A})$  generates adversarial observations  $\tilde{s}_t \sim \nu(s_t)$ . The perturbation is bounded by a budget  $\mathcal{B} : \mathcal{S} \rightarrow \mathcal{S}$ , limiting  $\text{supp } \nu(\cdot|s) \in \mathcal{B}(s)$ . For simplicity, we consider only zero-sum adversarial attacks, where the adversary minimizes the expected return of the victim. In case of *additive* perturbations  $\epsilon_t \in \mathcal{S}$  (Kumar et al., 2021),  $\nu(s_t) := \delta(\tilde{s}_t)$ . Here,  $\tilde{s}_t := s_t + \epsilon_t$ , and  $\tilde{s}_t$  are subject to a real positive episodic perturbation budget  $B \in \mathbb{R}$ . Given a victim policy  $\pi_v$ , this yields the following definition of an *optimal state-conditioned observation-space adversary*:

$$\nu^* = \arg \min_{\nu} \mathbb{E}_{\pi_v} \left[ \sum_{t=0}^{T-1} r_t \right] \quad \text{s. t.} \quad \sum_{t=0}^{T-1} \|\epsilon_t\|_2^2 \leq B^2, \quad (1)$$

where  $a_t \sim \pi_v(\cdot|\tilde{s}_t)$ ,  $\tilde{s}_t \sim \nu(s_t)$ ,  $s_{t+1} \sim t(\cdot|s_t, a_t)$ . In other words, given a fixed victim policy, the adversary seeks perturbations that minimise the victim return under the given budget constraints.

**Robustifying with co-training.** The optimal policy  $\pi_v^*$  in an SA-MDP thereby defines the optimal robust policy

of a victim under the presence of an optimal adversary  $\nu^*$ . To find such optimally robust victim policies, Zhang et al. (2021, ATLA) introduce a *co-training* approach to SA-MDPs, where the victim and the adversary are trained in turn while keeping the other’s policy fixed.

### 4. Illusory attacks

Unlike recent work on observation-space attacks (see Section 3), in this paper, we introduce observation-space attacks that aim to minimise detectability over sequences of observations. In addition, our framework does not require perturbation budget constraints, although these can be added for a fair comparison with prior literature (see Section 5).

#### 4.1. The illusory attack framework

The victim’s train-time policy  $\pi_v : \mathcal{S} \mapsto \mathcal{P}(\mathcal{A})$  is trained in an unattacked MDP  $\mathcal{E}$ . At test-time, the victim interacts with the *attacked MDP*  $\mathcal{E}'$ , i.e. the MDP containing the adversary, over a finite number of steps which may span multiple episodes. The victim has test-time access to a statistical detector  $\Delta$  which conditions on the victim’s total test-time experience  $\overline{\mathcal{H}}$ . Upon detecting the adversary, the victim may end test-time by triggering its contingency option  $\perp$ . We refer to the victim’s detector-augmented test-time policy as  $\overline{\pi}_v : \overline{\mathcal{H}} \mapsto \mathcal{P}(\mathcal{A} \cup \perp)$ .<sup>2</sup>

The adversary modifies the victim’s test-time observations and is aware of the victim’s test-time access to the detector  $\Delta$ . This embeds the adversary in a train-time setting that differs from the SA-MDP as the presence of the detector  $\Delta$  renders the setting non-Markovian. In Section 4.6 we transform this non-Markovian setting into an *Illusory MDP* ( $\mathcal{I}$ -MDP) by additionally conditioning  $\nu$  on the victim’s full test-time experience.

#### 4.2. Detecting illusory attacks

We now explore the limits of statistical detection. Within our illusory attack framework, an adversarial attack is detectable from empirical samples if and only if the *attacked MDP*  $\mathcal{E}'$ , which includes the adversary with  $\nu$ , is *statistically distinguishable* from the unattacked MDP  $\mathcal{E}$ .

**Definition 4.1** (Statistical indistinguishability). Let  $\mathcal{M} := \langle \mathcal{S}, \mathcal{A}, p, r, \gamma \rangle$  be an MDP with horizon  $T$ . Let  $\mathcal{Q}$  be a discrete stochastic control process (Bellman, 1957) that is not equivalent to  $\mathcal{M}$  in that it may not be fully observable, and may admit long-term correlations in its state-transition function<sup>3</sup>. Define  $\mathcal{Q}$ ’s observation space as  $\mathcal{Z} := \mathcal{S}$ , action space as  $\mathcal{A}$ , and fix its horizon at  $T$ . Let

<sup>2</sup>If the victim is chosen to be aware of  $\Delta$  at train-time, it can learn  $\pi_v$  such that  $\Delta$ ’s utility be maximised at test-time.

<sup>3</sup>Note that  $\mathcal{Q}$  is more general than a POMDP (Åström, 1965).

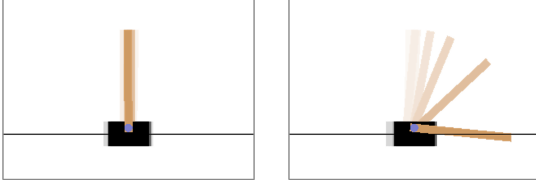


Figure 2: In *CartPole*, the agent aims to balance the brown pole by adjusting the position of the black cart. In the perfect illusory attack depicted above, the agents observations (left) appear unperturbed while the true system fails (right).

$\rho : \mathcal{S} \times (\mathcal{S} \times \mathcal{A})^{T-1} \mapsto \mathcal{P}(\mathcal{A})$  be a sampling policy that conditions on the entire action-observation history. Then  $\mathcal{Q}$  is *statistically indistinguishable* from  $\mathcal{M}$  under  $\rho$  if and only if  $\mathbb{P}_{\mathcal{M}, \rho}(\tau) = \mathbb{P}_{\mathcal{Q}, \rho}(\tau)$ .

Clearly, if  $\mathcal{E}$  is statistically indistinguishable from  $\mathcal{E}'$ , then it is impossible to construct a statistical detector that detects the presence of the adversary (see Section 4.1). Even if  $\mathcal{E}$  and  $\mathcal{E}'$  are statistically distinguishable, empirically estimating whether  $\mathbb{P}_{\mathcal{E}, \pi_v}(\tau) = \mathbb{P}_{\mathcal{E}', \pi_v}(\tau)$  may be sample-inefficient due to both the stochasticity of  $\mathcal{E}$  and the *curse of dimensionality* (Bellman, 1957). Instead, we propose to decompose the detection process into two steps:

**Theorem 4.2** (Testing MDP equivalence). *To determine whether a stochastic control process  $\mathcal{Q}$  is equivalent to a given Markov process  $\mathcal{M}$  under a policy  $\rho$ , it is sufficient to test both if  $\mathcal{Q}$ 's action-observation trajectories are consistent with the Markov property, i.e. are free of long-term correlations, and if  $\mathcal{Q}$ 's observation-transition function matches  $\mathcal{M}$ 's state-transition function (Shi et al. (2020)).*

Theorem 4.2 allows us to naturally trade off estimator sample-efficiency with detectability. We denote  $\Delta_1$  as a detector that checks only for state-transition consistency.  $\Delta_n$ ,  $n > 1$  then denotes a detector that checks both for state-transition consistency, as well as  $n$ -step correlations.

### 4.3. Undetectable adversarial attacks

We first introduce *perfect illusory attacks* which are undetectable as they leave  $\mathcal{E}$  and  $\mathcal{E}'$  statistically indistinguishable.

**Definition 4.3** (Perfect illusory attack). Consider two environments  $\mathcal{E}$  and  $\mathcal{E}'$  under a victim policy  $\pi_v$ , where  $\mathcal{E}$  is an adversary-free environment and  $\mathcal{E}'$  is attacked, i.e. subjected to an adversarial policy  $\nu$ . A perfect illusory attack is any adversarial policy  $\nu^\dagger$  that induces observation trajectories that differ from the underlying state transitions, while leaving  $\mathcal{E}$  and  $\mathcal{E}'$  *statistically indistinguishable* (Definition 4.1).

We provide examples of perfect illusory attacks in Section 5 as well as in the results video in the supp. material. Note that the definition of perfect illusory attacks (Definition 4.3)

makes no reference to the adversary's performance (victim reward). We, therefore, define *optimal* illusory attacks.

**Definition 4.4** (Optimal illusory attack). Let  $r_t$  be the victim reward. An optimal illusory attack  $\nu^*$  on  $(\mathcal{E}, \pi_v)$  is the family of perfect illusory attacks  $\nu^\dagger$  corresponding to the highest expected adversarial return, i.e.

$$\nu^* = \arg \min_{\nu^\dagger} \mathbb{E}_{\tau \sim \mathbb{P}(\mathcal{E}', \pi_v)} \left[ \sum_{t=0}^{T-1} r_t \right], \quad (2)$$

s.t.  $\mathbb{P}_{\mathcal{E}, \pi_v}(\tau) = \mathbb{P}_{\mathcal{E}', \pi_v}(\tau)$ ,

### 4.4. $\mathcal{E}$ -illusory attacks

Perfect illusory attacks do not always exist (see Appendix A.1) owing to their strict statistical indistinguishability constraints. We introduce  $\mathcal{E}$ -illusory attacks, which are a relaxation of optimal illusory attacks (see 4.4) that trade off detectability with versatility and can be learned end-to-end.

Instead of the full trajectory distributions,  $\mathcal{E}$ -illusory attacks only match the state-transition probabilities of attacked observations  $\tilde{s}$  with the unattacked MDP's state-transition function  $t$ . This implies that all transition tuples  $(\tilde{s}_t, a_t, \tilde{s}_{t+1})$  must be feasible under the state-transition function  $t$ . Note that, for simplicity, we assume that attacked observations all lie in the state space<sup>4</sup>, i.e.  $\tilde{s} \in \mathcal{S}$ .

**Definition 4.5** ( $\mathcal{E}$ -illusory attacks). An  $\mathcal{E}$ -illusory attack  $\nu_{\mathcal{E}}$  in  $\mathcal{E}'$  is an adversarial attack policy  $\nu$  (cf. Definition 4.4) that generates attacked observation transitions that are consistent with the state-transition function of the unattacked MDP  $\mathcal{E}$ . Formally,  $\forall \tilde{s}_t, a_t \sim \mathbb{P}(\mathcal{E}', \pi_v)$ ,

$$\nu_{\mathcal{E}} = \arg \min_{\nu} \mathbb{E}_{\tau \sim \mathbb{P}(\mathcal{E}', \pi_v)} \left[ \sum_{t=0}^{T-1} r_t \right], \quad (3)$$

s.t.  $t_{\mathcal{E}, \pi_v}(\cdot | \tilde{s}_t, a_t) = t_{\mathcal{E}', \pi_v}(\cdot | \tilde{s}_t, a_t)$ .

We note that consistency of attacked observation transitions with the unattacked environment's state-transition function alone *does not imply* the Markov property as it does not account for long-term correlations (see Appendix A.2 for an example). Hence,  $\mathcal{E}$ -illusory attacks in general *change the distribution* of trajectories, and can, in principle, be detected by victims with  $\Delta_n$  detectors when  $n > 1$ .

### 4.5. Adversaries trade off detectability and performance

In most environments, an adversary will need to trade off its expected adversarial return with the desire to avoid detection.

<sup>4</sup>Otherwise the victim could perform adversary detection based on observations alone (rather than observation transitions), which is not at the centre of our investigation.

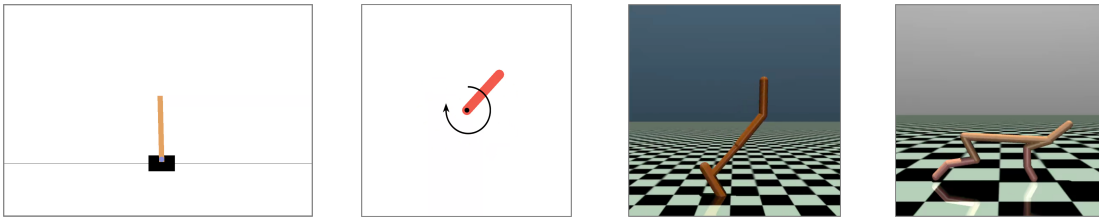


Figure 3: Benchmark environments used for empirical evaluation, from left to right. In *CartPole*, the agent has to balance a pole by moving the black cart. In *Pendulum*, the agent has to apply a torque action to balance the pendulum upright. In *Hopper* and *HalfCheetah*, the agent has to choose high-dimensional control inputs such that the agent moves towards the right of the image.

We hence define a relaxed form of Equation 3 with weighted adversarial objective  $\nu_{\mathcal{E}} = \arg \min_{\nu}$

$$\mathbb{E}_{\tau \sim \mathbb{P}(\mathcal{E}', \bar{\pi}_v)} \sum_{t=0}^{T-1} [r_t + \lambda \mathcal{D}(t_{\mathcal{E}, \pi_v}(\cdot | \tilde{s}_t, a_t), t_{\mathcal{E}', \bar{\pi}_v}(\cdot | \tilde{s}_t, a_t))], \quad (4)$$

where  $\lambda$  is a hyper-parameter that determines the weighing of the two objectives, and  $\mathcal{D}$  is a distance measure between probability distributions.

#### 4.6. Learning $\mathcal{E}$ -illusory attacks

Learning  $\mathcal{E}$ -illusory attacks from data end-to-end using reinforcement learning is complicated by the fact that the presence of the victim’s detector in  $\bar{\pi}_v$  renders the environment non-Markovian (cf. Section 4.1). We could model the adversary’s train-time environment as an MDP with non-Markovian reward function (Bacchus et al., 1996; Gaon & Brafman, 2019). However, this would not immediately allow for a principled application of reinforcement learning methods (Sutton & Barto, 2018).

We now show that the adversary’s train-time environment can instead be described as a *Illusory-MDP* ( $\mathcal{I}$ -MDP), which is a generalisation of the SA-MDP (Zhang et al., 2021) where the state contains the victim’s action-observation history. This allows us to use reinforcement learning techniques. We now give a formal definition of  $\mathcal{I}$ -MDPs.

**Definition 4.6** (Illusory MDP ( $\mathcal{I}$ -MDP)). Given a MDP  $\mathcal{E} := \langle \mathcal{S}, \mathcal{A}, p, r, \gamma \rangle$  with episode horizon  $T$  and a victim policy  $\bar{\pi}_v$ , an *Illusory MDP* ( $\mathcal{I}$ -MDP)  $\mathcal{E}_{\mathcal{I}} := \mathcal{I}(\mathcal{E}, \bar{\pi}_v)$  consists of a tuple  $\langle \hat{\mathcal{S}}, \hat{\mathcal{A}}, \hat{p}, \hat{r}, \gamma \rangle$  where  $\hat{\mathcal{A}} := \mathcal{S}$ ,  $\hat{\mathcal{S}} := \mathcal{S} \times (\hat{\mathcal{A}} \times \mathcal{A})^{T-1}$ ,  $\forall t$ ,

$$\begin{aligned} \hat{p}(\hat{s}_{t+1} | \hat{a}_t, \hat{s}_t) &= \bar{\pi}_v(a_t | \hat{a}_{<t}, a_{<t}) p(s_{t+1} | s_t, a_t), \\ \hat{r}(\hat{r}_{t+1} | \hat{s}_{t+1}, \hat{a}_t, \hat{s}_t) &= \bar{\pi}_v(a_t | \hat{a}_{\leq t}, a_{<t}) r(r_{t+1} | s_{t+1}, a_t, s_t). \end{aligned}$$

It immediately follows that the  $\mathcal{I}$ -MDP’s state is given by  $\hat{s}_t := (s_t, \hat{a}_{<t}, a_{<t})$ . Note that we assume zero-sum adversarial settings, therefore  $\hat{r}_{t+1} = -r_{t+1}$ . As the adversary’s

train-time environment is now expressed as an MDP, standard reinforcement learning methods can now be applied to Equation 4 by conditioning  $\nu$  on  $\hat{s}_t$ .

#### 4.7. Defending against illusory attacks

So far, we have assumed that the adversary corrupts all parts of the victim’s observation. However, in practice, the victim agent could receive a limited amount of unperturbed, *i.e.*, adversary free, environment observations through uncorruptable channels. We refer to such unattacked observation channels as *reality feedback*.

**Definition 4.7** (Reality feedback). We define reality feedback  $\zeta$  as a part of the victim’s observation  $\mathcal{Z}$  in  $\mathcal{E}'$  that cannot be corrupted by the adversary, *i.e.*, we assume that the victim’s observations  $\mathcal{Z} := \mathcal{Z}_0 \times \mathcal{Z}_{\zeta}$ , where the adversary can modify  $z^0 \in \mathcal{Z}_0$  but not  $z^{\zeta} \in \mathcal{Z}_{\zeta}$ .

As we show in Section 5, adversarial co-training can be used to robustify victim policies against illusory attacks in the presence of reality feedback.

### 5. Empirical evaluation of illusory attacks

We now compare and contrast perfect illusory attacks and  $\mathcal{E}$ -illusory attacks with state-of-the-art adversarial attacks, under the consideration of detectability, adversarial performance and possibilities of robustification. Our experiments show  $\mathcal{E}$ -illusory attacks are much less likely to be detected using  $\Delta_1$  detectors (Section 5.3) than state-of-the-art attacks, while perfect illusory attacks are undetectable. Similarly, in an IRB-approved study, we demonstrate that humans, in simple environments, efficiently detect state-of-the-art adversarial attacks but are considerably less likely to detect  $\mathcal{E}$ -illusory attacks (Section 5.4). We compare the reward performance of both prior attack frameworks and our novel illusory attacks, and investigate the effectiveness of state-of-the-art robustification methods (Section 5.6). We lastly investigate adversarial attacks with existence of unperturbed observation channels (reality feedback) in Section 5.7.

We provide the source code, a summary video, and individ-

---

**Algorithm 1**  $\mathcal{E}$ -illusory adversarial training

---

**Input:** environment  $env$  with transition function  $t$ , illusory reward weight  $\lambda$ , victim policy  $\pi_v$ , number of training episodes  $N$ .

Initialize adversary policy  $\nu_\psi$  with parameters  $\psi$ .

**while** episode < N **do**

$s_0 = env.reset()$

$\tilde{s}_0 = \nu_\psi(s_0)$

$a_0 = \pi_v(\tilde{s}_0)$

$s_1, r_1, done = env.step(a_0)$

$r_1^{adv} = -r_1$

$done = False$

**while** not  $done$  **do**

$a_t = \pi_v(\tilde{s}_t)$

$s_{t+1}, r_{t+1}, done = env.step(a_t)$

$r_{t+1}^{adv} = -r_{t+1} - \lambda \cdot \|\tilde{s}_t; t(\tilde{s}_{t-1}, a_{t-1})\|_\infty$

**end while**

    Update  $\nu_\psi$  from tuples  $(s_t, \tilde{s}_t, r_{t+1}^{adv}, s_{t+1})$ .

**end while**

---

ual videos per attack and random seed in the supplementary material. This ensures reproducibility and allows for qualitative comparison of different attack classes. We also provide detailed results with uncertainty statistics in Table A.5.1.

### 5.1. Experimental setup

We evaluate our methods on four standard benchmark environments (see Figure 3) with continuous state spaces whose dimensionalities range from 1 to 17 and both continuous and discrete action spaces. The mean and standard deviations of both detection and performance results are estimated from 200 independent episodes per each of 5 random seeds. Victim policies are pre-trained in unattacked environments, and frozen during adversary training. In line with Section 4.6, we assume the adversary has access to the unattacked environment’s state-transition function  $t$ .

### 5.2. Implementation details

**Perfect illusory attacks.** For all four evaluation environments, we succeed in implementing perfect illusory attacks (see Definition 4.3) by first constructing an attacked initial state distribution  $t(\cdot|\emptyset)$  that exploits environment-specific symmetries. We then sample the initial attacked observations  $\tilde{s}_0$  from the attacked initial state distribution and generate subsequent transitions using the unattacked state transition function  $t(\cdot|\tilde{s}_{t-1}, a_{t-1})$  where  $a_{t-1}$  is the action taken at the last time step. For details see also Appendix A.4.

**$\mathcal{E}$ -illusory attacks.** In contrast to perfect illusory attacks,  $\mathcal{E}$ -illusory attacks are learned end-to-end (see Section 4.6) using reinforcement learning. As detailed in Algorithm 1,

the adversary’s reward is given by the negative victim reward plus an *illusory reward* that incentivises attacked observations to be aligned with the unattacked state-transition function  $t$ . We choose the illusory reward to be proportional to the  $L_\infty$ -norm of the distance between the next state according to  $t$ , and the attacked observation. A hyperparameter  $\lambda$  trades off between victim reward and illusory reward. We ran a grid search over  $\lambda$  and found that for  $1 < \lambda < 1000$  results are mostly insensitive to  $\lambda$ , while  $\lambda < 1$  and  $\lambda > 1000$  result in either non-illusory attacks, or unattacked observations, respectively.

**State-of-the-art adversarial attacks.** We consider MNP (Kumar et al., 2021) and SA-MDP (Zhang et al., 2021) adversarial attacks together to be sufficiently representative of the state-of-the-art (see Section 3). Following recent works, we evaluate both MNP and SA-MDP attacks for perturbation budgets  $\beta \in \{0.05, 0.2\}$ , where  $\beta$  is defined relative to normalised observation vectors. For a fair comparison, we impose the same  $\beta$ s on  $\mathcal{E}$ -illusory attacks.

**Robustification.** We test the defenses *randomised smoothing (RS)* (Cohen et al., 2019; Kumar et al., 2021) and *adversarial pre-training (ATLA)* (Zhang et al., 2021). In RS, Gaussian noise is i.i.d. sampled at each time step and added to the victim’s observation  $\tilde{s}_t$ . In adversarial pre-training, the victim policy is learned through co-training with the adversary. In ATLA, the victim is co-trained with an SA-MDP adversary. We also consider an ablation of ATLA where we pre-train the victim agent with an  $\mathcal{E}$ -illusory adversary (which we refer to as *ATLA abl.*).

**Detectors.** For each of the four environments, we train a small neural network-based *world model* (Werbos, 2005; Ha & Schmidhuber, 2018)  $\hat{t}(\cdot|s, a)$  using trajectory rollouts from the unattacked environment. A world model approximates the environment’s state-transition function and can be used as an adversary detector  $\tilde{\Delta}_1$  (see Appendix A.3).  $\tilde{\Delta}_1$  uses  $\hat{t}$  to check whether, for a given observed transition  $(s_t, a_t, s_{t+1})$ ,  $\|\hat{t}(s_t, a_t); s_{t+1}\| \geq c$ . If so, the whole trajectory is classified as attacked. We evaluate  $\tilde{\Delta}_1$  on a held-out set of train-time trajectories and tune the detection threshold  $c$  to achieve a false positive (FP) rate of 3%.

### 5.3. Empirical detector evaluation

We now compare and contrast perfect illusory attacks,  $\mathcal{E}$ -illusory attacks, MNP attacks and SA-MDP attacks across different perturbation budgets  $\beta$ . We found results for  $\beta = 0.05$  to be comparable to those for  $\beta = 0.2$  and focus on  $\beta = 0.2$  in this analysis (see appendix for all results). As detailed in Figure 5, our detector  $\tilde{\Delta}_1$  detects MNP and SA-MDP attacks with a probability close to 100%. In contrast,

## Illusory Attacks

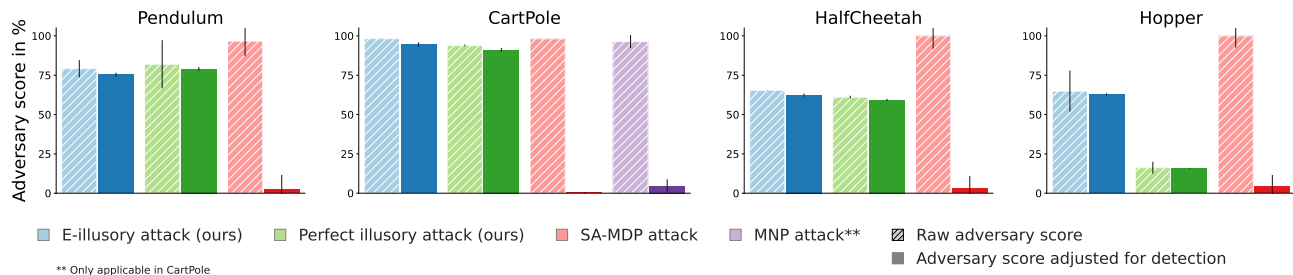


Figure 4: We display normalised adversary scores, indicating the reduction in the victim’s reward, on the y-axis. Each plot shows results in different environments, with different adversarial attacks on the x-axis. We show both the raw adversary score, as well as the adversary score adjusted for detection rates of different adversarial attacks (see Figure 5). While the SA-MDP and MNP benchmark attacks achieve higher unadjusted scores, their high detection rates result in significantly lower adjusted scores.

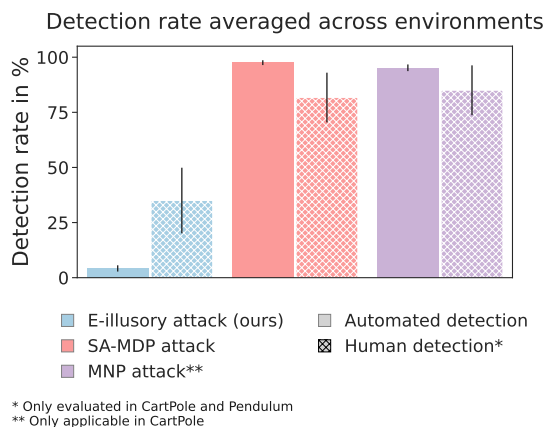


Figure 5: Different adversarial attacks are shown on the x-axis, with detection rates on the y-axis. We see that both the automated detector as well as human subjects are able to detect SA-MDP and MNP attacks, while  $\mathcal{E}$ -illusory attacks are less likely to be detected. Perfect illusory attacks are excluded here as they are undetectable.

the detector classifies  $\mathcal{E}$ -illusory attacks as adversarially attacked with very low probability. Note that perfect illusory attacks, as per definition, are undetectable and do not have a perturbation budget. In Figure 1, we illustrate why SA-MDP attacks can be detected with world models.

### 5.4. Detection by human inspection

We investigate whether humans unfamiliar with adversarial attacks detect adversarial attacks in the simple environments *CartPole* and *Pendulum*. To this end, we perform a controlled study with  $n = 10$  human participants. Participants were first shown an unattacked *introduction video* for both *CartPole* and *Pendulum*, exposing them to environment-specific dynamics. Participants were then shown a random set of videos containing both videos of unattacked

and attacked trajectories. For each video, participants were asked to indicate whether they believed that the video was unsuspecting, with the prompt “the system shown in the video was [not] the same as the one from the introduction video”. This phrasing was chosen so that participants would not be primed on the concept of illusory attacks (see Appendix A.6 for further details). Note that we restricted our study to the two benchmark environments with the shortest episodes, as we believe that these are more similar to real-world situations where humans perform sporadic inspection. We omit videos of perfect illusory attacks as these, by definition, cannot be detected.

We found that participants classified MNP and SA-MDP attacks as suspicious with high accuracy (see *Human detection* in Figure 5). In contrast, participants were almost equally likely to classify videos of unattacked and  $\mathcal{E}$ -illusory attacked trajectories as unsuspecting. In fact, at a confidence level of 95%, the hypothesis *participants are equally likely to classify an unattacked sequence as attacked as to classify an  $\mathcal{E}$ -illusory attacked sequence as attacked* cannot be rejected. Our findings suggest that humans are unable to detect  $\mathcal{E}$ -illusory attacks from short observation sequences in our simple environments. See Appendix A.6 for full results and the corresponding  $z$ -test statistic.

### 5.5. Comparative evaluation of adversary performance

**Relative adversary scores.** We now investigate the adversaries’ relative performance using the scalar *adversary score*. We define the *adversary score* as the resultant reduction in the victim’s return, normalised relative to both the best adversarial return in each class, as well as the victim’s expected return in the unattacked environment. We find that the adversary score – averaged across all environments – is generally higher for SA-MDP attacks than for  $\mathcal{E}$ -illusory attacks and *perfect illusory attacks* (see Figure 4). This is expected, as SA-MDP attacks purely minimise the victim

Attack	Normalised adversary score in %			
	no defence	smoothing	ATLA	ATLA abl.
MNP (Kumar et al., 2021)	96 ± 4	95 ± 1	-	-
SA-MDP (Zhang et al., 2021)	98 ± 7	68 ± 3	89 ± 6	93 ± 7
$\mathcal{E}$ -illusory attack (ours)	77 ± 7	65 ± 4	72 ± 4	72 ± 6
Perfect illusory attack (ours)	63 ± 8	71 ± 1	73 ± 7	23 ± 5

Table 1: Adversary scores and standard deviations averaged across environments for different defence methods and different attacks ( $\beta = 0.2$ ). Defences decrease the adversary score, i.e., increase the victim reward across all classes and all attack algorithms. We find that most defences only lead to marginal changes.

reward, while  $\mathcal{E}$ -illusory attacks trade off between minimizing the reward of the victim and remaining undetected. We further find that perfect illusory attacks achieve a lower adversary score than  $\mathcal{E}$ -illusory attacks. This is likewise to be expected, as perfect illusory attacks are not explicitly incentivised to lower the victim reward. MNP attacks, which can only be implemented in the discrete-action space environment *CartPole*, perform comparably to SA-MDP attacks. We hypothesize that the low score achieved by perfect illusory attacks in *Hopper* is because the foot motion is executed independently of the observation received.

**Detection-adjusted adversary scores.** We now adjust adversary scores to include the outcome of the automated detector by setting the adversary’s return to zero across episodes classified as attacked by  $\tilde{\Delta}_1$ . This reflects a middle ground across different scenarios in which adversary detection could trigger victim contingency options ranging from no action, to test-time termination, major security escalation, and adversary persecution. Specifically, we adjust the adversary score by multiplying it by  $1 - \mathbb{P}(\text{detection})$ . Figure 4 shows that  $\mathcal{E}$ -illusory attacks result in the highest average adversary score. In contrast, detection-adjusted adversary scores for state-of-the-art attacks are close to zero as expected from their high empirical detectability (see Fig. 5).

## 5.6. Comparative evaluation of robustification methods

We now investigate the effectiveness of different robustification methods against different adversarial attacks. As outlined in Section 5.1, we consider *randomized smoothing* (Kumar et al., 2021), *adversarial pretraining* (ATLA, (Zhang et al., 2021)) and an ablation of ATLA (ATLA abl.). We find that defences are generally more effective at restoring victim performance at  $\beta = 0.05$  (see app. A.5.1). Table 1 shows that for  $\beta = 0.2$  all defences result only in minor decrease in adversary score. With minor variations, these trends hold across all three robustification methods.

## 5.7. Robustification using reality feedback

We conclude our empirical investigations by exploring the importance of utilizing uncorrupted observation channels, which we refer to as *reality feedback* (see Definition 4.7). We establish two reality feedback scenarios for *CartPole*: one where the cart observation is unattacked, and one where the observation of the pole is unattacked. We find that robustifying the victim agent through adversarial training allows victim policies to use reality feedback effectively at test-time. Our results further suggest that having access to reality feedback channels allows for significant robustification if those channels are sufficiently *informative*. In the scenarios studied, we found that having access to an unattacked observation of the pole is more valuable than having access to an unattacked observation of the cart. See Appendix A.7 for further details.

## 6. Conclusion and future work

In this paper, we introduce *illusory attacks*, a novel class of adversarial attacks on sequential decision-makers that aim to reduce statistical detectability. Compared to state-of-the-art adversarial attacks, we show that both perfect and  $\mathcal{E}$ -illusory attacks are much harder to detect both by simple automated detection systems, and human supervisors.

We introduce illusory attacks for the purpose of increasing the security and safety of real-world systems. By definition, it is impossible to statistically detect perfect illusory attacks (see Definition 4.3). This implies that a successful real world defense strategy against such attacks has to ensure that the victim operates in an environment for which perfect illusory attacks are difficult, or impossible to perform.  $\mathcal{E}$ -illusory attacks differ from perfect illusory in that, in principle, they can be detected using multi-step detectors. Currently available detectors may not be sufficiently sample-efficient to provide adequate protection.

Our work shows that detectability should be a central consideration in future research on observation-space adversarial attacks. Future work should investigate not only the robustness of autonomous agents, but also the robustness of human-AI interaction systems to attacks that aim to minimise detection. To this end, more sample-efficient statistical detectors will need to be developed, and novel methods have to be devised that train agents to effectively use available uncorrupted observation channels for robustification.

Another avenue for future investigation is to understand in how far humans in human-in-the-loop systems detect adversarial attacks. We suggest that the human ability to perform “intuitive physics” (Hamrick et al., 2016), using robust but qualitative internal models of the world (Battaglia et al., 2013), may be central to this issue.



## Acknowledgements

We would like to thank Dr. Martin Strohmeier for helpful advice. This work is supported by the UKRI grant: Turing AI Fellowship EP/W002981/1 and EPSRC/MURI grant: EP/N019474/1. CS is generously sponsored by the Cooperative AI Foundation. This work benefitted from funding by armasuisse Science+Technology.

## References

- Andrychowicz, O. M., Baker, B., Chociej, M., Jozefowicz, R., McGrew, B., Pachocki, J., Petron, A., Plappert, M., Powell, G., Ray, A., et al. Learning dexterous in-hand manipulation. *The International Journal of Robotics Research*, 2020.
- Bacchus, F., Boutilier, C., and Grove, A. Rewarding behaviors. In *Proceedings of the thirteenth national conference on Artificial intelligence - Volume 2, AAAI'96*, pp. 1160–1167, Portland, Oregon, August 1996. AAAI Press. ISBN 978-0-262-51091-2.
- Bakhtin, A., Wu, D. J., Lerer, A., Gray, J., Jacob, A. P., Farina, G., Miller, A. H., and Brown, N. Mastering the game of no-press diplomacy via human-regularized reinforcement learning and planning. *arXiv preprint arXiv:2210.05492*, 2022.
- Battaglia, P. W., Hamrick, J. B., and Tenenbaum, J. B. Simulation as an engine of physical scene understanding. *Proceedings of the National Academy of Sciences*, 110(45):18327–18332, November 2013.
- Bellman, R. *Dynamic Programming*. Princeton University Press, 1957. ISBN 978-0-691-07951-6. Google-Books-ID: wdtoPwAACAAJ.
- Bellman, R. Dynamic programming and stochastic control processes. *Information and Control*, 1(3):228–239, September 1958. ISSN 0019-9958. doi: 10.1016/S0019-9958(58)80003-0.
- Brockman, G., Cheung, V., Pettersson, L., Schneider, J., Schulman, J., Tang, J., and Zaremba, W. Openai gym, 2016.
- Cazorla, L., Alcaraz, C., and Lopez, J. Cyber Stealth Attacks in Critical Information Infrastructures. *IEEE Systems Journal*, 12(2):1778–1792, June 2018. ISSN 1937-9234. doi: 10.1109/JSYST.2015.2487684. Conference Name: IEEE Systems Journal.
- Chen, T., Liu, J., Xiang, Y., Niu, W., Tong, E., and Han, Z. Adversarial attack and defense in reinforcement learning from AI security view. *Cybersecurity*, 2019.
- Cohen, J., Rosenfeld, E., and Kolter, Z. Certified adversarial robustness via randomized smoothing. In *International Conference on Machine Learning*. PMLR, 2019.
- Degrave, J., Felici, F., Buchli, J., Neunert, M., Tracey, B., Carpanese, F., Ewalds, T., Hafner, R., Abdolmaleki, A., de Las Casas, D., et al. Magnetic control of tokamak plasmas through deep reinforcement learning. *Nature*, 602(7897):414–419, 2022.

- Dennis, M., Jaques, N., Vinitzky, E., Bayen, A., Russell, S., Critch, A., and Levine, S. Emergent complexity and zero-shot transfer via unsupervised environment design. *Advances in neural information processing systems*, 33: 13049–13061, 2020.
- Everett, M., Lutjens, B., and How, J. P. Certifiable Robustness to Adversarial State Uncertainty in Deep Reinforcement Learning. *IEEE Transactions on Neural Networks and Learning Systems*, 2021.
- Fu, H., Liu, W., Wu, S., Wang, Y., Yang, T., Li, K., Xing, J., Li, B., Ma, B., Fu, Q., et al. Actor-critic policy optimization in a large-scale imperfect-information game. In *International Conference on Learning Representations*, 2022.
- Gaon, M. and Brafman, R. I. Reinforcement Learning with Non-Markovian Rewards, December 2019.
- Goodfellow, I. J., Shlens, J., and Szegedy, C. Explaining and harnessing adversarial examples. *arXiv preprint arXiv:1412.6572*, 2014.
- Ha, D. and Schmidhuber, J. World Models. March 2018. doi: 10.5281/zenodo.1207631.
- Haarnoja, T., Zhou, A., Abbeel, P., and Levine, S. Soft actor-critic: Off-policy maximum entropy deep reinforcement learning with a stochastic actor. In *International conference on machine learning*. PMLR, 2018.
- Hamrick, J. B., Battaglia, P. W., Griffiths, T. L., and Tenenbaum, J. B. Inferring mass in complex scenes by mental simulation. *Cognition*, 157:61–76, 2016.
- Huang, S., Papernot, N., Goodfellow, I., Duan, Y., and Abbeel, P. Adversarial attacks on neural network policies. *arXiv preprint arXiv:1702.02284*, 2017.
- Huang, Y. and Zhu, Q. Deceptive reinforcement learning under adversarial manipulations on cost signals. In *International Conference on Decision and Game Theory for Security*, pp. 217–237. Springer, 2019.
- Hussenot, L., Geist, M., and Pietquin, O. Copycat: Taking control of neural policies with constant attacks. *arXiv preprint arXiv:1905.12282*, 2019.
- Ilahi, I., Usama, M., Qadir, J., Janjua, M. U., Al-Fuqaha, A., Hoang, D. T., and Niyato, D. Challenges and countermeasures for adversarial attacks on deep reinforcement learning. *IEEE Transactions on Artificial Intelligence*, 3(2):90–109, 2021.
- Kingma, D. P. and Ba, J. Adam: A method for stochastic optimization. *arXiv preprint arXiv:1412.6980*, 2014.
- Kos, J. and Song, D. Delving into adversarial attacks on deep policies. *arXiv preprint arXiv:1705.06452*, 2017.
- Kumar, A., Levine, A., and Feizi, S. Policy Smoothing for Provably Robust Reinforcement Learning. Technical report, arXiv, 2021.
- Lanctot, M., Zambaldi, V., Gruslys, A., Lazaridou, A., Tuyls, K., Pérolat, J., Silver, D., and Graepel, T. A unified game-theoretic approach to multiagent reinforcement learning. *Advances in neural information processing systems*, 30, 2017.
- Langner, R. Stuxnet: Dissecting a Cyberwarfare Weapon. *IEEE Security & Privacy*, 9(3):49–51, May 2011. ISSN 1558-4046. doi: 10.1109/MSP.2011.67. Conference Name: IEEE Security & Privacy.
- Lanier, J. B., McAleer, S., Baldi, P., and Fox, R. Feasible adversarial robust reinforcement learning for underspecified environments. *arXiv preprint arXiv:2207.09597*, 2022.
- Li, S., Neupane, A., Paul, S., Song, C., Krishnamurthy, S. V., Chowdhury, A. K. R., and Swami, A. Adversarial Perturbations Against Real-Time Video Classification Systems. In *Proceedings 2019 Network and Distributed System Security Symposium*, 2019.
- Liang, Y., Sun, Y., Zheng, R., and Huang, F. Efficient adversarial training without attacking: Worst-case-aware robust reinforcement learning. In *Advances in Neural Information Processing Systems*, 2022.
- Lin, Y.-C., Liu, M.-Y., Sun, M., and Huang, J.-B. Detecting adversarial attacks on neural network policies with visual foresight. *arXiv preprint arXiv:1710.00814*, 2017.
- McAleer, S., Lanier, J., Wang, K., Baldi, P., Fox, R., and Sandholm, T. Self-play psro: Toward optimal populations in two-player zero-sum games. *arXiv preprint arXiv:2207.06541*, 2022a.
- McAleer, S., Wang, K., Lanctot, M., Lanier, J., Baldi, P., and Fox, R. Anytime optimal psro for two-player zero-sum games. *arXiv preprint arXiv:2201.07700*, 2022b.
- McAleer, S., Farina, G., Lanctot, M., and Sandholm, T. Escher: Eschewing importance sampling in games by computing a history value function to estimate regret. *International Conference on Learning Representations*, 2023.
- Mnih, V., Kavukcuoglu, K., Silver, D., Rusu, A. A., Veness, J., Bellemare, M. G., Graves, A., Riedmiller, M., Fidjeland, A. K., Ostrovski, G., et al. Human-level control through deep reinforcement learning. *nature*, 2015.

- Mo, Y. and Sinopoli, B. False data injection attacks in control systems. In *Preprints of the 1st workshop on Secure Control Systems*, volume 1, 2010.
- Oikarinen, T., Zhang, W., Megretski, A., Daniel, L., and Weng, T.-W. Robust deep reinforcement learning through adversarial loss. *Advances in Neural Information Processing Systems*, 34, 2021.
- Pasqualetti, F., Dorfler, F., and Bullo, F. Control-theoretic methods for cyberphysical security: Geometric principles for optimal cross-layer resilient control systems. *IEEE Control Systems Magazine*, 35(1):110–127, 2015.
- Perolat, J., De Vylder, B., Hennes, D., Tarassov, E., Strub, F., de Boer, V., Muller, P., Connor, J. T., Burch, N., Anthony, T., et al. Mastering the game of stratego with model-free multiagent reinforcement learning. *Science*, 378(6623): 990–996, 2022.
- Qiaoben, Y., Ying, C., Zhou, X., Su, H., Zhu, J., and Zhang, B. Understanding Adversarial Attacks on Observations in Deep Reinforcement Learning. Technical report, arXiv, 2021.
- Raffin, A., Hill, A., Gleave, A., Kanervisto, A., Ernestus, M., and Dormann, N. Stable-baselines3: Reliable reinforcement learning implementations. *Journal of Machine Learning Research*, 22(268):1–8, 2021.
- Salimans, T., Ho, J., Chen, X., Sidor, S., and Sutskever, I. Evolution strategies as a scalable alternative to reinforcement learning. *arXiv preprint*, 2017.
- Schulman, J., Wolski, F., Dhariwal, P., Radford, A., and Klimov, O. Proximal Policy Optimization Algorithms. Technical report, arXiv, August 2017.
- Shi, C., Wan, R., Song, R., Lu, W., and Leng, L. Does the Markov Decision Process Fit the Data: Testing for the Markov Property in Sequential Decision Making, February 2020. arXiv:2002.01751 [cs, stat].
- Sokota, S., D’Orazio, R., Kolter, J. Z., Loizou, N., Lanctot, M., Mitliagkas, I., Brown, N., and Kroer, C. A unified approach to reinforcement learning, quantal response equilibria, and two-player zero-sum games. *arXiv preprint arXiv:2206.05825*, 2022.
- Sun, J., Zhang, T., Xie, X., Ma, L., Zheng, Y., Chen, K., and Liu, Y. Stealthy and Efficient Adversarial Attacks against Deep Reinforcement Learning, May 2020. arXiv:2005.07099 [cs].
- Sun, Y., Zheng, R., Liang, Y., and Huang, F. Who is the strongest enemy? towards optimal and efficient evasion attacks in deep rl. In *International Conference on Learning Representations*, 2021.
- Sutton, R. S. The Quest for a Common Model of the Intelligent Decision Maker, June 2022.
- Sutton, R. S. and Barto, A. G. *Reinforcement Learning: An Introduction*. A Bradford Book, Cambridge, MA, USA, 2018. ISBN 978-0-262-03924-6.
- Szegedy, C., Zaremba, W., Sutskever, I., Bruna, J., Erhan, D., Goodfellow, I., and Fergus, R. Intriguing properties of neural networks. *arXiv preprint arXiv:1312.6199*, 2013.
- Tekgul, B. G., Wang, S., Marchal, S., and Asokan, N. Real-time attacks against deep reinforcement learning policies. *arXiv preprint arXiv:2106.08746*, 2021.
- Todorov, E., Erez, T., and Tassa, Y. MuJoCo: A physics engine for model-based control. In *2012 International Conference on Intelligent Robots and Systems*, 2012.
- Vinyals, O., Babuschkin, I., Czarnecki, W. M., Mathieu, M., Dudzik, A., Chung, J., Choi, D. H., Powell, R., Ewalds, T., Georgiev, P., et al. Grandmaster level in starcraft ii using multi-agent reinforcement learning. *Nature*, 575 (7782):350–354, 2019.
- Werbos, P. J. Applications of advances in nonlinear sensitivity analysis. In *System Modeling and Optimization: Proceedings of the 10th IFIP Conference New York City, USA, August 31–September 4, 1981*. Springer, 2005.
- Wu, F., Li, L., Huang, Z., Vorobeychik, Y., Zhao, D., and Li, B. CROP: Certifying Robust Policies for Reinforcement Learning through Functional Smoothing. *ArXiv*, 2021.
- Zhang, H., Chen, H., Xiao, C., Li, B., Liu, M., Boning, D., and Hsieh, C.-J. Robust Deep Reinforcement Learning against Adversarial Perturbations on State Observations. In *Advances in Neural Information Processing Systems*. Curran Associates, Inc., 2020.
- Zhang, H., Chen, H., Boning, D., and Hsieh, C.-J. Robust Reinforcement Learning on State Observations with Learned Optimal Adversary, January 2021.
- Åström, K. J. Optimal Control of Markov Processes with Incomplete State Information I. *Journal of Mathematical Analysis and Applications*, 1965.

## A. Appendix

### A.1. Proof on the existence of perfect illusory attacks

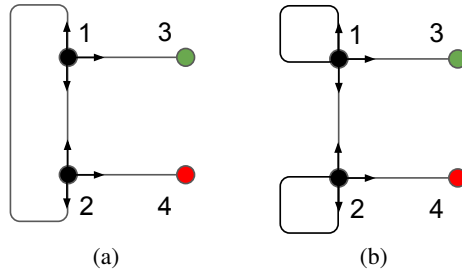


Figure 6: An environment for which perfect illusory attacks do exist (left), and one for which they do not exist (right).

*Proof that perfect illusory attacks exist.* We consider an example MDP (see Figure 6a) where a victim starts in node 1 or 2 each with probability  $\frac{1}{2}$  and can go *up*, *down*, or *right* in both states 1 and 2. The episode terminates immediately with a return of 0 should the victim reach state 4. Otherwise, the victim receives a reward of +1 if it reaches state 3 within a maximum of 2 steps. The optimal victim policy is therefore to take paths  $1 \rightarrow 3$  if starting in state 1, and take one of the two possible paths  $2 \rightarrow 1 \rightarrow 3$  otherwise. The victim observes the labelled state graph, as well as its current state label. Clearly, choosing  $\nu(1) = 2$  and  $\nu(2) = 1$  constitutes a perfect illusory attack in this environment.  $\square$

*Proof that perfect illusory attacks don't always exist.* To show that some environments do not admit perfect illusory attacks, consider the modified environment in Figure 6b. Here, clearly a timestep-conditioned victim policy that takes the action sequence  $\langle \text{up}, \text{right} \rangle$  independently of observations cannot be perfectly attacked.  $\square$

### A.2. Two stochastic processes can have the same states and state-transition function, but not be equal



Figure 7: Left: An unattacked Markov Decision Process with 6 states. Right: A decision process with the same state-transition function, but long-term correlations.

Two stochastic processes can have the same states and state-transition functions, but still not be equal. Figure 7 illustrates this with a simple example: The attacked process on the right transitions to state  $E$  whenever it has been in  $B$  prior, and transitions to  $F$  whenever it has been in  $C$  prior. This process has the exact state-transition function as the process on the left, hence cannot be distinguished from it using a  $\Delta_1$  detector. However, a  $\Delta_2$  detector could distinguish both processes.

### A.3. Detector used in experiments

We assume that the victim is trained in the unperturbed MDP  $\mathcal{M}_{\text{unp}}$  for  $k$  episodes of length  $n$ . During training, the agent records the observed environment transition tuples  $t_i = (s_i, a_i, s_{i+1})$  and stores these in a set  $\mathcal{D}_{\text{unp}} = \{t_i\}_{i=0}^{i=k*(n-1)}$ . We use the set of unperturbed transitions  $\mathcal{D}_{\text{unp}}$  to learn an approximate dynamics model  $\hat{t}(s_t | s_{t-1}, a_{t-1})$ . We implement  $\hat{t}$  as a Multi-Layer-Perceptron with two hidden layers of size 10, and train the model with an  $l_2$  loss for 10 epochs, using a learning rate of 0.001 and the ADAM optimizer (Kingma & Ba, 2014). We then evaluate the model on a held-out set of the training observations and tune a threshold  $c$  to achieve a false positive rate of 3%. We then use  $c$  as a threshold to detect adversarial attacks. We evaluate the accuracy in detecting adversarial attacks for all scenarios listed in Table A.5.1. More specifically, at every time step, the victim uses the detector to predict the next observation given the previous observation

and action taken. If the  $l_2$  distance between the predicted observation and the actual (adversarial) observation is larger than the threshold  $c$ , the victim classifies the episode as adversarially attacked. Results for this detection mechanism are given in Table A.5.1.

#### A.4. Perfect illusory attacks implementation

We implemented perfect illusory attacks in *CartPole*, *Pendulum* by setting the first observation  $\bar{s}_0$  to the negative of the true first state sampled from the environment, i.e.  $\bar{s}_0 = -s_0$ . Note that in *HalfCheetah* and *Hopper* the initial state distribution is not centered around zero, we hence accounted for this by first subtracting the offset, then computing the negative of the observation and re-adding the offset. As the distribution over initial states is symmetric in all environments (after removing the offset), this approach of generating adversarial attacks satisfies the conditions of a perfect illusory attack (see Definition 4.3). We provide videos of the generated perfect illusory attacks in the supplementary material in the respective folder and show an illustration of a perfect illusory attack in Figure 2.

#### A.5. Learning $\mathcal{E}$ -illusory attacks with reinforcement learning

We next describe the algorithm used to learn  $\mathcal{E}$ -illusory attacks and the training procedures used to compute the results in Table A.5.1. We use the *CartPole*, *Pendulum*, *HalfCheetah* and *Hopper* environments as given in Brockman et al. (2016). We shortened the episodes in *Hopper* and *HalfCheetah* to 300 steps to speed up training. The transition function is implemented using the physics engines given in all environments. We normalise observations by the maximum absolute observation. We train the victim with PPO (Schulman et al., 2017) and use the implementation of PPO given in Raffin et al. (2021), while not making any changes to the given hyperparameters. In both environments we train the victim for 1 million environment steps. We implement the ATLA (Zhang et al., 2021) victim by co-training it with an adversary agent, and follow the original implementation of the authors<sup>5</sup>. We implement the ablation of ATLA (Zhang et al., 2021) that trains the victim with an illusory adversary by merely replacing the SA-MDP adversary with an  $\mathcal{E}$ -illusory attack adversary, which is implemented as stated in algorithm 1. For co-training, we alternate between training the victim and the adversary agent every 400 environment steps. This parameter was chosen in a small evaluation study as it yields non-oscillating behaviour. We further investigated different ratios between training steps of the adversary and training steps of the victim, but found that a ratio of one, i.e. equal training of both, yields the most stable results for co-training.

We implement the illusory adversary agent with SAC (Haarnoja et al., 2018), where we likewise use the implementation given in Raffin et al. (2021). We initially ran a small study and investigated four different algorithms as possible implementations for the adversary agent, where we found that SAC yields best performance and training stability.

We train all adversarial attacks for three million environment steps. We implemented randomized smoothing as a standard defence against adversarial attacks on RL agents, as introduced in Kumar et al. (2021). We use the author’s original implementation<sup>6</sup>.

In future work we will investigate applying state-of-the-art deep RL algorithms for finding Nash equilibria in two-player zero-sum games such as PSRO-based methods (Lanctot et al., 2017; McAleer et al., 2022b;a; Vinyals et al., 2019) or regret-based methods (McAleer et al., 2023; Perolat et al., 2022; Fu et al., 2022; Sokota et al., 2022) to find  $\mathcal{E}$ -illusory attacks.

##### A.5.1. RESULTS FOR PERTURBATION BUDGET $\beta = 0.05$

We show the remaining results for a perturbation budget of  $\beta = 0.05$  in Figures 8 and 9, and in Table 2. Note that the corresponding Figures in the main paper are for a perturbation budget of  $\beta = 0.2$ .

<sup>5</sup>[https://github.com/huanzhang12/ATLA\\_robust\\_RL](https://github.com/huanzhang12/ATLA_robust_RL)

<sup>6</sup><https://openreview.net/forum?id=mwdfai8NBrJ>

## Illusory Attacks

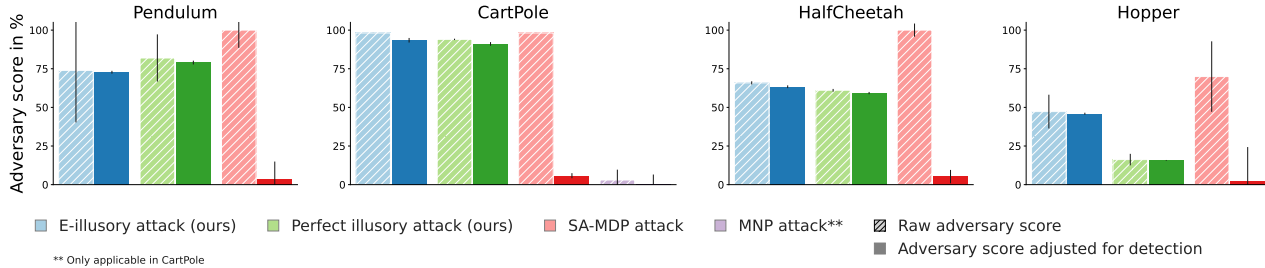


Figure 8: Results for  $\beta = 0.05$ . We display normalised adversary scores, indicating the reduction in the victim’s reward, on the y-axis. Each plot shows results in different environments, with different adversarial attacks on the x-axis. We show both the raw adversary score, as well as the adversary score adjusted for detection rates of different adversarial attacks (see Figure 5). While the SA-MDP and MNP benchmark attacks achieve higher unadjusted scores, their high detection rates result in significantly lower adjusted scores. Note that MNP attacks perform significantly worse for  $\beta = 0.05$ , as compared to  $\beta = 0.2$  (see Figure 4).

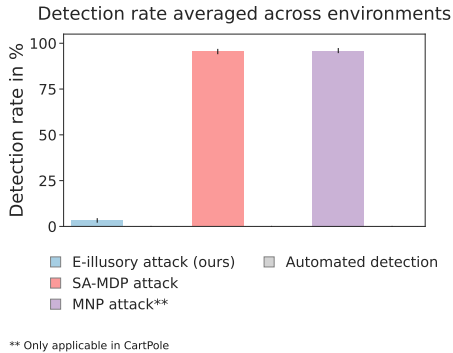


Figure 9: Results for  $\beta = 0.05$ . Different adversarial attacks are shown on the x-axis, with detection rates on the y-axis. We see that the automated reliably detector detects SA-MDP and MNP attacks, while  $\mathcal{E}$ -illusory attacks are less likely to be detected. Perfect illusory attacks are excluded here as they are undetectable. Note that the study with human subjects did not contain examples with  $\beta = 0.05$ .

Attack	Normalised adversary score in %			
	no defence	smoothing	ATLA	ATLA abl.
MNP (Kumar et al., 2021)	3 ± 6.7	64 ± 7	-	-
SA-MDP (Zhang et al., 2021)	92 ± 13	53 ± 14	91 ± 11	89 ± 8
$\mathcal{E}$ -illusory attack (ours)	71 ± 18	50 ± 11	81 ± 32	75 ± 11
Perfect illusory attack (ours)	63 ± 8	71 ± 1	73 ± 7	23 ± 5

Table 2: Adversary scores and standard deviations averaged across environments for different defence methods and different attacks ( $\beta = 0.05$ ). Defences decrease the adversary score, i.e., increase the victim reward across all classes and all attack algorithms.

### A.5.2. VIDEOS OF ALL ADVERSARIAL ATTACKS

We provide a video summarising results in the supplementary material. Further, we provide videos for different seeds for all adversarial attacks in the supplementary material. The folders are named respectively. All videos were generated for a budget  $\beta = 0.2$ .

### A.6. Human study

**Study approval.** Our study was approved by an independent ethics committee under reference R84123/RE001.

**Setup.** We performed a controlled experiment with  $n = 10$  human participants. All participants were graduate-level university students, while none had prior knowledge about the objective of the study. Participants participated voluntarily; we estimate the time needed per participant to be around 15 minutes. Participants were handed a slide show which contained all relevant information. This slide show is included in the supplementary material in the respective folder. We further add the sheet with ground truth labels for all video sequences.

After consenting to participate, participants were provided with the slide show and an online sheet to indicate their answers.

## Illusory Attacks

Table 3: Full results table for all four environments

attack	budget $\beta$	Detection rate [%]		Victim reward under different defences			
		naive	ATLA <sup>3</sup>	none	smoothing	ATLA	ATLA abl.
<b>Pendulum</b>							
SA-MDP (Zhang et al., 2021)	0.05	96.2± 0.01	95.4± 0.02	-797.2± 69.9	-408.4± 146.6	-757.2± 109.3	-722.2± 30.8
$\mathcal{E}$ -illusory attack (ours)		1.6± 0.01	2.1± 0.01	-638.8± 204.6	-387.8± 115.8	-634.4± 370.4	-634.9± 103.9
SA-MDP (Zhang et al., 2021)	0.2	97.7± 0.01	93.8± 0.02	-1387.0± 119.0	-1188.3± 70.4	-1354.6± 107.1	-1428.3± 91.5
$\mathcal{E}$ -illusory attack (ours)		4.9± 0.01	4.7± 0.01	-1170.1± 67.5	-940.2± 91.6	-1020.4± 50.0	-1029.4± 106.7
Perfect illusory attack (ours)	1	3.6± 0.01	3.4± 0.01	-1204.8± 88.6	-1231.7± 25.3	-1284.5± 158.5	1228.6± 50.0
unattacked		3.2± 0.01	3.5± 0.01	-189.4			
<b>CartPole</b>							
MNP (Kumar et al., 2021)	0.05	96.0± 0.01		485.0± 33.5	180.3± 33.6		
SA-MDP (Zhang et al., 2021)		94.1± 0.02	94.5± 0.02	9.4± 0.2	122.5± 54.3	24.2± 7.3	16.8± 8.3
$\mathcal{E}$ -illusory attack (ours)		4.8± 0.01	4.6± 0.01	9.3± 0.1	165.4± 46.3	21.4± 6.0	45.4± 56.5
MNP (Kumar et al., 2021)	0.2	95.2± 0.02		18.3± 20.8	20.8± 8.7		
SA-MDP (Zhang et al., 2021)		99.7± 0.01	96.0± 0.01	9.3± 0.1	39.0± 10.7	9.2± 0.1	9.7± 0.6
$\mathcal{E}$ -illusory attack (ours)		3.7± 0.01	5.8± 0.02	9.0± 0.3	23.9± 3.3	9.6± 0.6	10.0± 1.20
Perfect illusory attack (ours)	1	3.1± 0.01	3.6± 0.01	30.1± 2.2	25.0± 1.6	21.9± 12.8	19.1± 4.6
unattacked		3.1± 0.01	3.3± 0.01	500.0			
<b>HalfCheetah</b>							
SA-MDP (Zhang et al., 2021)	0.05	94.8± 0.02	94.9± 0.02	-1570.8± 177.4	101.3± 71.7	-570.2± 156.8	-625.3± 312.6
$\mathcal{E}$ -illusory attack (ours)		3.8± 0.01	4.7± 0.01	-149.1± 41.8	103.1± 44.8	-67.4± 47.3	-117.2± 2.3
SA-MDP (Zhang et al., 2021)	0.2	97.1± 0.01	92.2± 0.02	-1643.8± 344.8	-36.8± 8.9	-1443.9± 313.8	-1200.7± 175.1
$\mathcal{E}$ -illusory attack (ours)		4.7± 0.01	4.3± 0.01	-178.9± 4.6	-31.0± 8.2	-64.7± 32.6	-35.5± 21.90
Perfect illusory attack (ours)	1	3.3± 0.01	3.4± 0.01	5.9± 36.8	-33.8± 4.7	153.0± 138.9	125.4± 107.5
unattacked		3.1± 0.01	3.5± 0.01	2594.6			
<b>Hopper</b>							
SA-MDP (Zhang et al., 2021)	0.05	96.8± 0.01	96.4± 0.01	144.1± 265.4	488.5± 66.4	-205.7± 148.7	-124.0± 152.0
$\mathcal{E}$ -illusory attack (ours)		2.9± 0.01	6.2± 0.02	408.0± 127.2	489.5± 58.5	-79.4± 192.6	140.3± 69.4
SA-MDP (Zhang et al., 2021)	0.2	95.6± 0.02	94.6± 0.02	-761.5± 127.4	255.1± 28.9	-274.8± 96.1	-502.6± 209.4
$\mathcal{E}$ -illusory attack (ours)		3.5± 0.01	3.9± 0.01	-157.5± 225.3	238.2± 24.8	-108.0± 106.6	-84.9± 176.4
Perfect illusory attack (ours)	1	3.2± 0.01	3.4± 0.01	679.2± 63.9	239.3± 32.9	59.5± 161.9	78.7± 165.6
unattacked		3.4± 0.01	3.0± 0.01	958.1			

The study was self-paced and done by the participants without further supervision. We further advised participants not to do the study if they would not feel comfortable at any point in time.

The first 18 videos in the slide show are 100-frame long sequences of the *Pendulum* environment, i.e. six each for either no adversarial attack, an  $\mathcal{E}$ -illusory attack or an SA-MDP attack (Zhang et al., 2021). The subsequent 24 10-frame long sequences of the *CartPole* include the same attacks as for *Pendulum*, plus an additional six sequences under an MNP attack (Kumar et al., 2021). Note that MNP attacks cannot be applied to the *Pendulum* environment, as it has a continuous action space. For all attacks, the budget  $\beta$  was 0.2. Within both groups, the order of the videos shown was randomised. Subjects had to choose for each video between *correct* and *false*, where *false* indicates that subjects find that the system observed in the respective video is not the same as the one observed in the introductory video. We likewise refer to a video marked as *false* as a *suspicious* video. Table 5 includes all empirically estimated probabilities and standard deviations for classifying a segment from a given class as *false*.

**Result analysis.** We find that subjects reported one-third of unattacked sequences as *false*. Subjects classified sequences under an MNP or SA-MDP (Zhang et al., 2020) attack as *false* with a probability higher than 80%, while categorizing illusory attacks as *false* with a probability of only 32.4%. We computed the double-sided z-statistics and were able to reject both the hypothesis that  $P(\text{false} \mid \text{SA-MDP})=P(\text{false} \mid \text{no attack})$  and the hypothesis that  $P(\text{false} \mid \text{MNP})=P(\text{false} \mid \text{no attack})$  for

## Illusory Attacks

Table 4: Reward achieved by victim for different reality feedback scenarios.

Reality feedback	Victim agent	
	naive	ATLA abl.
Pole	$9.84 \pm 0.1$	$182.44 \pm 36.9$
Cart	$8.83 \pm 0.3$	$15.54 \pm 6.6$

Table 5: Results from our study with human participants.

	Environment		
	both	Pendulum	CartPole
$P(\text{false} \mid \text{no attack})$	$34.2 \pm 11.4$	$31.5 \pm 10.5$	$37.0 \pm 12.3$
$P(\text{false} \mid \text{SA-MDP})$	$81.4 \pm 27.2$	$96.3 \pm 32.1$	$66.7 \pm 22.2$
$P(\text{false} \mid \mathcal{E}\text{-illusory attack})$	$32.4 \pm 10.8$	$37.0 \pm 12.3$	$27.7 \pm 9.3$
$P(\text{false} \mid \text{MNP})$	$83.3 \pm 27.8$		$83.3 \pm 27.8$

$\alpha = 0.05$ , while the hypothesis that  $P(\text{false} \mid \mathcal{E}\text{-illusory attack}) = P(\text{false} \mid \text{no attack})$  cannot be rejected. We conclude that subjects were able to distinguish SA-MDP and MNP attacks from unattacked sequences while being unable to distinguish illusory attacks from unattacked sequences.

### A.7. Reality feedback

**Setup.** We evaluate the importance of realism feedback in the *CartPole* environment by investigating two possible scenarios. Note that the observation in *CartPole* is given as a four-dimensional vector of the pole angle and angular velocity, as well as cart position and velocity. In the first test scenario, the victim correctly observes the pole, while the adversary can perturb the observation of the cart; the second scenario is vice versa. We investigate two test cases for each scenario: First, attacking a naive victim, and second, attacking an agent pretrained with co-training.

**Results and discussion.** Table 4 shows that the reward achieved by the victim is generally higher when pretrained with co-training. We hypothesize that this pretraining enables the agent to learn how to utilize the reality feedback effectively. The achieved victim performance when reality feedback contains information about the *pole* is more than 10 times larger than when containing information on the *cart* instead. This seems intuitive, as the observation of the pole appears much more useful for the task of stabilizing the pole, and underlines the importance of equipping agents with strong reality feedback channels.